Dispersion Characteristics of the Broadside-Coupled Coplanar Waveguide

Cam Nguyen, *Senior Member, IEEE*

Abstract— **The dispersive properties for the even- and odd-modes of the broadside-coupled coplanar waveguide (CPW) are determined using the spectral domain method. Various numerical results of the even- and odd-mode effective dielectric constants as a function of frequency are presented and discussed. It is found that the structure has a very weak dispersion. This fact is further confirmed through a comparison between the calculated dynamic and quasi-static results of the even- and odd-mode effective dielectric constants. The low dispersion feature signifies the fact that the quasi-static analysis is adequate for designing practical microwave and millimeter-wave circuits employing broadside-coupled CPW.**

I. Introduction

A broadside-coupled structure using coplanar waveguide (CPW) techniques, suitable for broad-band microwave integrated circuits (MIC's) and microwave monolithic integrated circuits (MMIC's) has been developed [1]–[3]. This structure has inherent wide-band and tight-coupling characteristics as well as a large ratio between the even- and odd-mode phase velocities. The latter feature is very attractive for designing compact microwave filters because multipole stop-band and multizero pass-band responses can be obtained by a single filter section, as demonstrated for the broadside-coupled stripline [4]. Furthermore, the use of CPW in realizing the broadside-coupled transmission line produces additional desirable features for both MIC and MMIC applications, resulting from the top-surface ground planes, such as elimination of via holes for ground connections, ease in realizing compact balanced circuits, minimization of cross talk, and easy and accurate on-wafer RF measurements. Recently, end-coupled band-pass filters using the broadside-coupled CPW have been reported [3]. So far, the propagation characteristics of broadside-coupled CPW have only been studied using quasi-static methods [1]–[3]. Its dispersion characteristics have not been investigated.

In this paper, an analysis and investigation for the dispersive properties of the broadside-coupled CPW are presented for the first time. The full-wave analysis, which is based on the spectral domain method (SDM) [5], produces accurately the dispersion characteristics of both the fundamental even- and odd-modes. It is discovered that the broadside-coupled CPW possesses a very low dispersion in comparing with the conventional broadside-coupled stripline [6]. This unique characteristic is very useful since a simple quasi-static TEM approach can be employed for accurate circuit designs in the high-frequency region. This fact is confirmed by a good agreement between the dynamic and quasi-static numerical results of the even- and odd-mode effective dielectric constants. Further, the weak dispersion property is indeed very attractive for wide-band applications.

Manuscript received May 20, 1993.

C. Nguyen is with the Department of Electrical Engineering, Texas A&M University, College Station, TX 77843–3128.

IEEE Log Number 9211846.

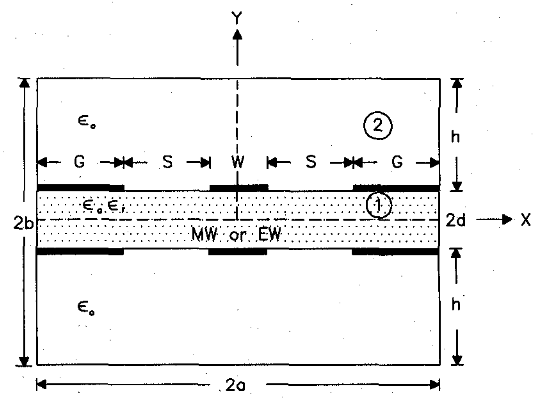

Fig. 1. A cross section of the broadside-coupled CPW.

II. Formulation

The broadside-coupled CPW, as shown in Fig. 1, is analyzed. The structure is enclosed in a perfectly conducting channel and assumed to be uniform and infinite in the z-direction. Both the ground planes and central strip are assumed to be perfectly conducting and infinitely thin, and the dielectric substrate is assumed to be lossless. In this structure, there exists two propagation modes, the even- and odd-modes corresponding to an open-circuit [magnetic wall (MW)] and a short-circuit [electrical wall (EW)], respectively, a the center of the dielectric substrate. They are both fundamental modes, corresponding to E_z even-E_x odd (with respect to x). Sketches of the electric field configurations for these modes are given in Fig. 2. In view of the symmetry we only need to consider one half of the cross section, as shown in Fig. 1. Since the SDM formulation is well established [5], here we will describe only the essential steps.

The even- and odd-modes existing in the considered structure can be classified as hybrid modes, consisting of both TE and TM fields. By introducing the scalar electric, Ψ^e, and magnetic, Ψ^h, potentials associated with the TM and TE modes, respectively we can express the fields in each region

0018–9480/93$03.00 © 1993 IEEE

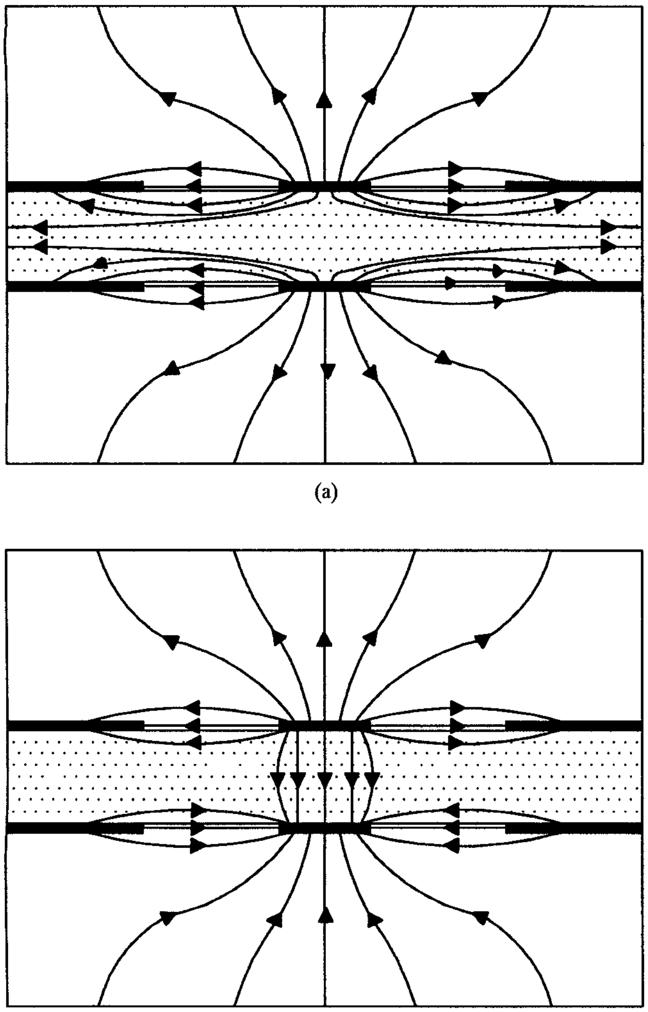

(a)

(b)

Fig. 2. Electric field configurations for the even mode (a) and odd mode (b) of the broadside-coupled CPW.

$i, i = 1, 2$, in the spectral domain as follows,

$$\tilde{E}_{xi}(\alpha_n, y) = -j\alpha_n \tilde{\Psi}_i^e(\alpha_n, y) + \frac{\omega\mu_i}{\beta}\frac{\partial\tilde{\Psi}_i^h(\alpha_n, y)}{\partial y} \quad (1)$$

$$\tilde{E}_{yi}(\alpha_n, y) = j\,\frac{\alpha_n\omega\mu_i}{\beta}\,\tilde{\Psi}_i^h(\alpha_n, y) + \frac{\partial\tilde{\Psi}_i^e(\alpha_n, y)}{\partial y} \quad (2)$$

$$\tilde{E}_{zi}(\alpha_n, y) = j\,\frac{k_i^2 - \beta^2}{\beta}\,\tilde{\Psi}_i^e(\alpha_n, y) \quad (3)$$

$$\tilde{H}_{xi}(\alpha_n, y) = -j\alpha_n \tilde{\Psi}_i^h(\alpha_n, y) - \frac{\omega\varepsilon_i}{\beta}\frac{\partial\tilde{\Psi}_i^e(\alpha_n, y)}{\partial y} \quad (4)$$

$$\tilde{H}_{yi}(\alpha_n, y) = -j\,\frac{\alpha_n\omega\varepsilon_i}{\beta}\,\tilde{\Psi}_i^e(\alpha_n, y) + \frac{\partial\tilde{\Psi}_i^h(\alpha_n, y)}{\partial y} \quad (5)$$

$$\tilde{H}_{zi}(\alpha_n, y) = j\,\frac{k_i^2 - \beta^2}{\beta}\,\tilde{\Psi}_i^h(\alpha_n, y) \quad (6)$$

where ω is the radian frequency, β is the propagation constant, $k_i = \omega\sqrt{\varepsilon_i\mu_i}$ is the wave number; and $\alpha_n = (n - 1/2)(\pi/a)$, $n = 1, 2, \cdots,$, is the Fourier-transform variable. The factor $e^{j(wt-\beta z)}$ is suppressed. The tilde ($\tilde{}$) indicates the Fourier-transformed quantity in accordance to

$$\tilde{f}(\alpha_n, y) = \int_{-a}^{a} f(x, y)e^{j\alpha_n x}\,dx \quad (7)$$

$\tilde{\Psi}_i^e$ and $\tilde{\Psi}_i^h$ are the solutions of the Fourier-transformed Helmholtz equation

$$\frac{\partial^2\tilde{\Psi}_i^{e,h}(\alpha_n, y)}{\partial y^2} - \gamma_i^2\tilde{\Psi}_i^{e,h}(\alpha_n, y) = 0, \quad (8)$$

$$\gamma_i^2 = \alpha_n^2 + \beta^2 - k_i^2$$

which are given, for the even mode, as

$$\tilde{\Psi}_1^e(\alpha_n, y) = A^e(\alpha_n)\cosh\gamma_1 y \quad (9)$$

$$\tilde{\Psi}_1^h(\alpha_n, y) = A^h(\alpha_n)\sinh\gamma_1 y \quad (10)$$

$$\tilde{\Psi}_2^e(\alpha_n, y) = B^e(\alpha_n)\sinh[\gamma_2(b - y)] \quad (11)$$

$$\tilde{\Psi}_2^h(\alpha_n, y) = B^h(\alpha_n)\cosh[\gamma_2(b - y)] \quad (12)$$

where $A^{e,h}$ and $B^{e,h}$ are unknown constants. For the odd mode, $\cosh\gamma_1 y \leftrightarrow \sinh\gamma_1 y$. These potentials already satisfy the boundary conditions at the perfectly conducting wall at $y = b$, magnetic wall at $y = 0$ (even-mode), and electrical wall at $uy = 0$ (odd-mode). The fields in the spectral domain in the two regions can now be derived by substitution of (9)–(12) into (1)–(6).

We now apply the remaining boundary conditions at the dielectric interface ($y = d$) in the spectral domain, obtained as Fourier transforms of those in the space domain, and Galerkin's method along with Parseval's theorem. The result is the following set of coupled linear algebraic equations

$$\sum_{m=0}^{M} P_{11}^{pm}(\beta)c_m + \sum_{k=1}^{K} P_{12}^{pk}(\beta)d_k = 0, \quad p = 0, 1, \cdots, M \quad (13)$$

$$\sum_{m=0}^{M} P_{21}^{qm}(\beta)c_m + \sum_{k=1}^{K} P_{22}^{qk}(\beta)d_k = 0, \quad q = 1, 2, \cdots, K \quad (14)$$

where

$$P_{11}^{pm} = \sum_{n=1}^{N} \tilde{E}_{xp}(\alpha_n)\tilde{G}_{11}(\alpha_n, \beta)\tilde{E}_{xm}(\alpha_n) \quad (15)$$

$$P_{12}^{pk} = \sum_{n=1}^{N} \tilde{E}_{xp}(\alpha_n)\tilde{G}_{12}(\alpha_n, \beta)\tilde{E}_{zk}(\alpha_n) \quad (16)$$

$$P_{21}^{qm} = \sum_{n=1}^{N} \tilde{E}_{zq}(\alpha_n)\tilde{G}_{21}(\alpha_n, \beta)\tilde{E}_{xm}(\alpha_n) \quad (17)$$

$$P_{22}^{qk} = \sum_{n=1}^{N} \tilde{E}_{zq}(\alpha_n)\tilde{G}_{22}(\alpha_n, \beta)\tilde{E}_{zk}(\alpha_n) \quad (18)$$

c_m and d_k are unknown coefficients, associated with the respective Fourier-transformed known basis functions E_{xm} and E_{zk} that describe the x and z slot field distributions at the interface, respectively. It is noted that the slot field components E_{xm} and E_{zk} must be chosen of that they are nonzero only at the slots. N represents the number of the spectral terms.

G_{11}, G_{12}, G_{21}, and G_{22} are the dyadic Green's function in the spectral domain; they are given for the even mode by

$$\tilde{G}_{11} = \frac{-j}{\omega\mu_0}\left\{(k_1^2 - \beta^2)\frac{\tanh\gamma_1 d}{\gamma_1} + (k_0^2 - \beta^2)\frac{\coth\gamma_2 h}{\gamma_2}\right\} \tag{19}$$

$$\tilde{G}_{12} = \tilde{G}_{21} = -\frac{j\alpha_n\beta}{\omega\mu_0}\left\{\frac{\tanh\gamma_1 d}{\gamma_1} + \frac{\coth\gamma_2 h}{\gamma_2}\right\} \tag{20}$$

$$\tilde{G}_{22} = \frac{-j}{\omega\mu_0}\left\{(k_1^2 - \alpha_n^2)\frac{\tanh\gamma_1 d}{\gamma_1} + (k_0^2 - \alpha_n^2)\frac{\coth\gamma_2 h}{\gamma_2}\right\} \tag{21}$$

where k_o is the free-space wave number. For the odd mode, $\tanh\gamma_1 d \leftrightarrow \coth\gamma_1 d$.

The propagation constants, β, and, hence, the effective dielectric constants, $\varepsilon_{eff} = (\beta/k_0)^2$, can now be obtained by solving the determinantal equation of the coefficient matrix of (13) and (14).

III. Numerical Results

The numerical efficiency of the solution process and the accuracy of the solutions depends strongly on the choice of the basis functions, E_{xm} and E_{zk}. First, computation time can be reduced significantly if the chosen basis functions resemble the actual physical behavior of the slot field distributions and have closed-form Fourier transforms. Second, the basis functions should belong to a complete set, so that the solution accuracy can be enhanced by increasing the number of basis functions. And, lastly, they should be twice continuously differentiable to avoid spurious solutions [7]. To meet these criteria, we have employed the following basis functions [5] in our computations:

$$E_{xm}(x) = \begin{cases} \dfrac{\cos[m\pi(2x+W+S)/2S]}{\sqrt{1-[(2x+W+S)/S]^2}} - \dfrac{\cos[m\pi(2x-W-S)/2S]}{\sqrt{1-[(2x-W-S)/S]^2}}, \\ \quad m = 0, 2, \cdots, M \\ \dfrac{\sin[m\pi(2x+W+S)/2S]}{\sqrt{1-[(2x+W+S)/S]^2}} - \dfrac{\sin[m\pi(2x-W-S)/2S]}{\sqrt{1-[(2x-W-S)/S]^2}}, \\ \quad m = 1, 3, \cdots, M \end{cases} \tag{22}$$

$$E_{zk}(x) = \begin{cases} \dfrac{\cos[k\pi(2x+W+S)/2S]}{\sqrt{1-[(2x+W+S)/S]^2}} - \dfrac{\cos[k\pi(2x-W-S)/2S]}{\sqrt{1-[(2x-W-S)/S]^2}}, \\ \quad k = 1, 3, \cdots, K \\ \dfrac{\sin[k\pi(2x+W+S)/2S]}{\sqrt{1-[(2x+W+S)/S]^2}} - \dfrac{\sin[k\pi(2x-W-S)/2S]}{\sqrt{1-[(2x-W-S)/S]^2}}, \\ \quad k = 2, 4, \cdots, K \end{cases} \tag{23}$$

which are defined only over the slots.

Figs. 3 and 4 shows calculated values of the effective dielectric constants for the even- and odd-modes as a function of frequency with the strip width and slot with as a parameter, respectively. It is apparent from these figures that the mode effective dielectric constants are almost insensitive with changes in the frequency, even though a high dielectric constant substrate (Alumina) is used. This discovered unique phenomenon demonstrates that the broadside-coupled CPW is very weakly dispersive, and, thus, is very attractive for MIC's and MMIC's as compared to the conventional broadside-coupled stripline, whose dispersion is large [6]. The low dispersion characteristics also indicate that the quasi-static results [1]–[3] are adequate for circuit designs, employing broadside-coupled CPW, in the high-frequency regime. Furthermore, it is seen in Fig. 3 that as the strip width is increased, the even- and odd-mode effective dielectric constants are decreased and increased, respectively, producing an increasing ratio for the effective dielectric constants. In Fig. 4, it is clear that increasing the slot width reduces the even-mode effective dielectric constant while maintains virtually constant the odd-mode effective dielectric constant. Consequently, one can obtain a large ratio for the mode effective dielectric constants by using a large slot. The large mode effective-dielectric-constant ratio feature is very useful for miniaturized filter applications.

Quasi-static results for the even- and odd-mode effective dielectric constants, obtained in [3], are also shown in Fig. 3 and 4. As can be seen, they agree well with the dynamic

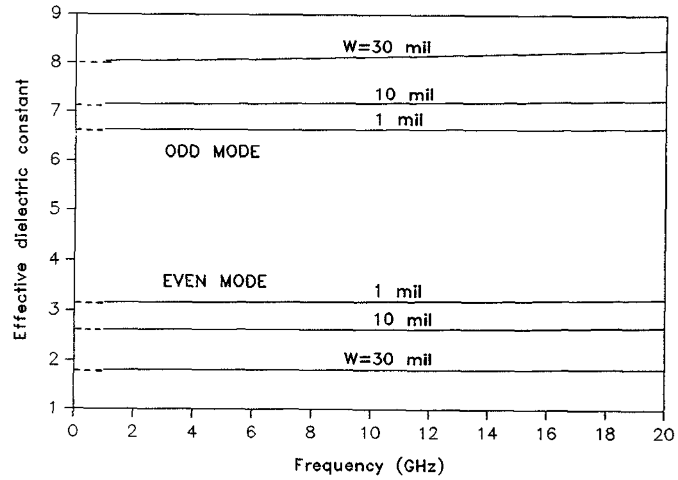

Fig. 3. Even- and odd-mode effective dielectric constants of the broadside-coupled CPW as a function of frequency (with strip width as a parameter). $2a = 100$ mil, $h = 20$ mil, $2d = 5$ mil, $\varepsilon_r = 10.5$ (Alumina), $S = 20$ mil. - - -: quasi-static results [3].

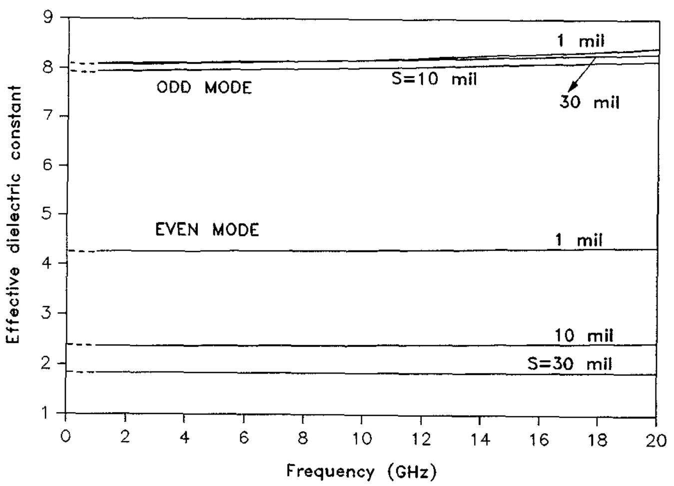

Fig. 4. Even- and odd-mode effective dielectric constants of the broadside-coupled CPW as a function of frequency (with slot width as a parameter). $2a = 100$ mil, $h = 20$ mil, $2d = 5$ mil, $\varepsilon_r = 10.5$ (Alumina), $W = 20$ mil. - - -: quasi-static results [3].

data, as expected, due to the weak dispersion properties of the broadside-coupled CPW.

Numerous variations of results for the mode effective dielectric constants versus numbers of basis functions and spectral terms have also been investigated to determine the convergence of the solutions. Our convergence investigations have indicated that, for dimensions used in most practical circuits, 200 spectral terms and 2 basis functions give sufficient accuracy for engineering purposes.

IV. Conclusions

The dispersion characteristics of the broadside-coupled CPW have been formulated using the spectral domain technique. Numerical results for the even- and odd-mode effective dielectric constants have been presented, including the convergence behavior. It has been found that this CPW structure possesses very small dispersion characteristics, which confirm the adequacy of the quasi-static analysis for high-frequency circuit design purposes. It has also been shown that a large ratio for the mode effective dielectric constants can be obtained by increasing the strip or slot width. The discovered weak dispersion, together with the inherent features of broadband, tigh-coupling and large mode velocity ratio, make the broadside-coupled CPW very attractive for MIC and MMIC applications.

References

[1] T. Hatsuda, "Computation of coplanar-type strip-line characteristics by relaxation method and application to microwave circuits," *IEEE Trans. Microwave Theory Tech.,* vol. MTT-23, no. 10, pp. 795–802, Oct. 1975.
[2] S. S. Bedair and I. Wolff, "Fast and accurate analytic formulas for calculating the parameters of a general broadside-coupled coplanar waveguide for (M)MIC applications," *IEEE Trans. Microwave Theory Tech.,* vol. MTT-37, no. 5, pp. 843–850, May 1989.
[3] C. Nguyen, Broadside-Coupled Coplanar Waveguides and Their End-Coupled Band-Pass Filter Applications," *IEEE Trans. Microwave Theory Tech.,* vol. MTT-40, no. 12, pp. 2181–2189, Dec. 1992.
[4] J. L. Allen, "Inhomogeneous coupled-line filters with large mode-velocity ratios," *IEEE Trans. Microwave Theory Tech.,* vol. MTT-22, no. 12, pp. 1182–1186, Dec. 1974.
[5] T. Uwano and T. Itoh, "Spectral Domain Approach," in *Numerical Techniques for Microwave and Millimeter-Wave Passive Structures,* T. Itoh, Ed. New York: Wiley, 1989.
[6] K. Kawano, "Hybrid-mode analysis of a broadside-coupled microstrip line," *IEEE Proc.,* vol. 131, pt. H, no. 1, pp. 21–24, Feb. 1984.
[7] R. H. Jansen, "High speed computation of single and coupled microstrip parameters including dispersion, higher order modes, loss and finite strip thickness," *IEEE Trans. Microwave Theory Tech.,* vol. MTT-26, no. 10, pp. 75–87, 1978.

Cam Nguyen, (S'82–M'83–SM'91) for a biography, see this issue p. 1488.